

Phonon-Assisted Recombination of Free Excitons in Compound Semiconductors

B. SEGALL AND G. D. MAHAN

General Electric Research and Development Center, Schenectady, New York 12301

(Received 7 February 1968)

In this paper we study the band-edge optical transitions in "direct" semiconductors involving the interacting exciton-phonon system, especially the longitudinal-optical (LO)-phonon-assisted recombination of free excitons. By introducing an extended Green's-function approach to include propagation in and between the various bands in the exciton spectrum, we obtain rather directly the transition rate to lowest order in the exciton-photon coupling which contains the effects of the interactions between the exciton and lattice vibrations to all orders, and thus includes line broadening, shift, asymmetry, and all renormalizations. Under the appropriate conditions (sufficiently separated bands), this result is equivalent to an expression previously derived by Toyozawa, but has the virtue that all terms appearing in it (in particular, the asymmetry term) are given in precise and general expressions. The relation of the general result to that obtained by conventional perturbation theory is discussed. The radiative decay of free excitons by the one-LO- and two-LO-phonon-assisted processes are formulated in the framework of perturbation theory. The limitation of this approach and its relationship to that in which the exciton-photon interaction is treated more accurately are briefly discussed. It is also shown that the second-order perturbation-theory result for the one-phonon-assisted processes (both for absorption and emission), including the contributions from the full intermediate state (hydrogenic) spectrum, can be evaluated exactly in closed form. The one- and two-LO-phonon-assisted emission spectra for CdS are calculated for several temperatures up to 77°K using only experimentally determined parameters and taking the anisotropy of the valence band into account. Except for the one-LO peak at $T=77^{\circ}\text{K}$, where the polariton effects are important, the calculated line shapes and widths, as well as the intensity ratio of peaks, are found to be in good accord with the observed spectra. The corresponding calculations for ZnO at 77°K are in good agreement with experimental spectrum. The zero-LO exciton peak due to the one-acoustic-phonon-assisted process is calculated in weak exciton-photon coupling approximations for both the deformation potential and piezoelectric couplings. The widths of the calculated lines are orders of magnitude smaller than the observed widths, and we conclude that the difficulty lies in the use of the weak exciton-photon coupling approach.

I. INTRODUCTION

TO achieve a proper understanding of the optical properties of nonmetallic crystals, it is necessary to take account of the exciton states. This fact has been well understood for a long time for the insulators like the alkali halides, where the absorption is dominated by very strong exciton peaks. The understanding of the important role played by excitons in semiconductors, particularly those compound semiconductors with moderate to reasonably large band gaps, has come somewhat more recently; but it has, in fact, been in the compound semiconductors that our knowledge of the exciton system has been elucidated most extensively and in the greatest detail. Noteworthy here are the investigations of the optical absorption and reflectivity in CdS¹ and in other II-VI semiconducting compounds² which have been carried out over the past several years. In addition to the information about the intrinsic exciton system, these studies have been the principal source of our present information about the electronic structure of these materials. These studies have also contributed to the understanding of the exciton-phonon coupling and its effect on the absorption and relatedly on the reflectivity.

On the other hand, considerably less work has been reported on the emission properties of the intrinsic excitons. This is because even in the purest presently available crystals, the low-temperature fluorescence spectra are dominated by processes involving various crystal imperfections. It has been only rather recently, in fact, that the radiative recombination of a free exciton (at the exciton "resonant" energy) and of the exciton with the simultaneous emission of one or more longitudinal optical (LO) phonons have been definitively identified.³ The first detailed experimental investigation of the shape of these peaks for a range of temperatures has been carried out by Gross *et al.*⁴ in CdS crystals. These results were the impetus for the theoretical work to be reported in this paper.⁵

Figure 1 is taken from Gross *et al.*⁴ and gives the emission spectra of a CdS single crystal at $T=4.2$ and 42°K. At the lower temperature the very large peaks are associated with exciton recombinations at defects. On the

³ C. E. Bleil and I. Broser, in *Proceedings of Seventh International Conference on the Physics of Semiconductors* (Dunod Cie., Paris, 1964), p. 897; C. E. Bleil, *J. Phys. Chem. Solids* **27**, 1631 (1966); R. Rass, doctoral dissertation, Free University of Berlin, 1965 (unpublished).

⁴ E. Gross, S. Permogorov, and B. Razbirin, *J. Phys. Chem. Solids* **27**, 1647 (1966); *Fiz. Tverd. Tela* **8**, 1483 (1966) [English transl.: *Soviet Phys.—Solid State* **8**, 1180 (1966)].

⁵ Preliminary reports of this work appeared in B. Segall and G. D. Mahan, *Bull. Am. Phys. Soc.* **12**, 364 (1967); G. D. Mahan and B. Segall, in *Proceedings of International Conference on II-VI Semiconducting Compounds, Providence, R. I.* (W. A. Benjamin, Inc., New York, 1967), p. 349.

¹ D. G. Thomas and J. J. Hopfield, *Phys. Rev.* **116**, 573 (1959); J. J. Hopfield and D. G. Thomas, *ibid.* **122**, 35 (1961).

² A recent survey of this work is given in B. Segall and D. T. F. Marple, in *The Physics and Chemistry of II-IV Compounds*, edited by M. Aven and J. S. Prener (North-Holland Publishing Co., Amsterdam, 1967), Chap. 7.

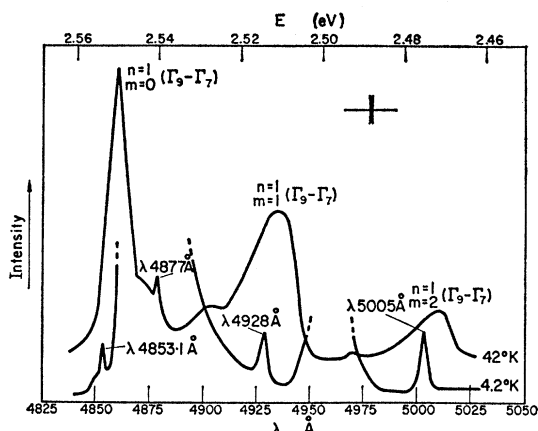


FIG. 1. CdS emission spectra at 4.2 and 42°K observed by Gross *et al.* (reproduced with permission from Ref. 4). These spectra exhibit peaks due to the radiative decay of "free" A exciton with and without LO phonon cooperation.

other hand, the weak peak at 2.5546 eV ($\lambda=4853.1 \text{ \AA}$) lies almost precisely at the resonant energy for the $n=1$ exciton state of the A (the lowest energy) exciton series E_{x1}^A , as determined by the low-temperature reflectivity studies.¹ The energies of the other weak peaks in the figure at 4928 and 5005 \AA correspond quite closely to $E_{x1}^A - \hbar\omega_1$ and $E_{x1}^A - 2\hbar\omega_1$, where $\hbar\omega_1$ is the LO-phonon energy near the zone center. This suggests that these emissions are recombinations with the simultaneous emission of one-LO and two-LO phonons. As the temperature is raised, the intensities of these three emission lines increase relative to those associated with the defects and at 42°K are much stronger than the latter. This is consistent with the above interpretation, since as the temperature is raised there is an increasing probability for the excitons to dissociate from the defects into the exciton bands. Further evidence lending support to the identification is that the peaks have nearly Maxwellian shapes, and the widths at moderately low temperatures ($T \lesssim 60^\circ\text{K}$) are roughly equal to $k_B T$. These are consequences of the thermal distribution $\exp(-\hbar^2 K^2 / 2M k_B T)$ of "free" excitons in the "initial" states (within the 1S band), as noted by Gross *et al.*⁴ These authors further suggested on the basis of qualitative arguments that the transition probabilities $P_m(\omega)$, as a function of photon energy $\hbar\omega$, for the processes involving m LO phonons is

$$P_m(\omega) \propto \Delta_m^{(5/2)-m} \exp(-\Delta_m/k_B T), \quad (1.1)$$

with

$$\Delta_m = \hbar\omega + m\hbar\omega_1 - E_{x1} \quad (m=1, 2). \quad (1.2)$$

In this paper we calculate in detail the emission spectra for the one-LO- and two-LO-phonon-assisted processes using a weak-coupling approximation for both the exciton-photon and exciton-phonon interactions. Among other things, we check the validity of (1.1). The calculation is simplified by noting that under the reasonable assumption of quasithermal equilibrium for the

excitons the emission process is the inverse of the phonon-assisted absorption, a process which has been studied earlier. Also, from this relation and the role of LO-assisted absorption in "wide" band-gap semiconductors² (e.g., II-IV compounds), it can be seen that the LO-assisted emission will be important in this class of materials. These transitions have just recently been identified in ZnO and CdSe.⁶ In addition to their general occurrence, these transitions have taken on added importance, since it has been shown that they can undergo stimulated emission.⁶⁻⁸

For these calculations, as well as related problems, it is important to have a general theory for the optical transition probability for the coupled exciton-phonon system. Two approaches have been used to extend the theory beyond the weak-coupling approximation for both interactions. In the one discussed by Hopfield⁹ the interaction between the exciton and photon is treated accurately, leading to the so-called "polariton" states—the eigenstates of the interacting exciton-photon system. The exciton-phonon coupling is then taken into account by perturbation theory. As Hopfield has emphasized, unless the exciton-photon coupling is very weak, it is essential to take into account the polariton effects in optical transitions around the resonance energy. In the other approach, which has been studied most extensively by Toyozawa,¹⁰ higher-order contributions from the exciton-phonon coupling are calculated, while only the lowest-order terms in the exciton-photon interaction are retained. By use of a generalized damping theory, Toyozawa has obtained for the transition rate for absorption at frequency ω , $W(\omega)$, the expression

$$W(\omega) = \frac{1}{\pi\omega} \sum_{\lambda} |\tilde{M}_{\lambda}|^2 \frac{\tilde{\Gamma}_{\lambda}(0, \omega) + 2\tilde{C}_{\lambda}(\omega)(\omega - \tilde{\epsilon}_{\lambda, 0})}{(\omega - \tilde{\epsilon}_{\lambda, 0})^2 + \tilde{\Gamma}_{\lambda}(0, \omega)^2}. \quad (1.3)$$

Here the quantum numbers pertaining to the relative motion of the exciton are designated by λ , \mathbf{K} is center of mass momentum, $\tilde{\epsilon}_{\lambda, \mathbf{K}}$ is the exciton energy, $\tilde{\Gamma}_{\lambda}(\mathbf{K}=0, \omega)$ is the width, and \tilde{M}_{λ} is the optical matrix element. The tilde (\sim) indicates that the quantity is renormalized by self-energy effects. The result, aside from incorporating linewidth and energy of shifts due to exciton-phonon coupling, contains a term (the second in the numerator) which introduces an asymmetry in the exciton line. Toyozawa did not derive a general expression for the factor $\tilde{C}_{\lambda}(\omega)$ in this term, although he did give an approximate expression for it.

⁶ J. R. Packard, D. A. Campbell, and W. C. Tait, *J. Appl. Phys.* **38**, 5255 (1967).

⁷ L. A. Kulevsky and A. M. Prokhorov, *IEEE J. Quant. Electron.* **QE-2**, 584 (1966); L. N. Kurbatov, V. E. Mashchenko, and N. N. Mochalkin, *Opt. i Spektroskopiya* **22**, 429 (1967) [English transl.: *Opt. Spectry. (USSR)* **22**, 232 (1967)].

⁸ C. Benoit a la Guillaume, J. M. Debever, and F. Salvan, in *Proceedings of the International Conference on II-VI Semiconducting Compounds, Providence, R. I.* (W. A. Benjamin, Inc., New York, 1967), p. 669.

⁹ J. J. Hopfield, *Phys. Rev.* **112**, 1555 (1958).

¹⁰ Y. Toyozawa, *J. Phys. Chem. Solids* **25**, 59 (1964).

In Sec. II we will derive the result (1.3) by a Green's-function approach. Aside from being more direct and somewhat more general, the approach provides a derivation for $\tilde{C}_\lambda(\omega)$ and gives expressions for the renormalized matrix elements. The relationship of these more general results to those obtained by conventional perturbation theory will be discussed.

In Sec. III we discuss the LO-phonon-assisted radiative decay of excitons. Account will be taken of the large anisotropy of the valence bands of the wurtzite compounds. We note that in the second-order perturbation calculation for the one-LO-phonon-assisted process, there occurs a sum over the complete spectrum (including both discrete and continuum states) of internal exciton states. In the related absorption problems, this sum has either been approximated by the lowest ($n=1$) state alone or has been carried out by some other approximate procedure. We will show that this sum can be obtained exactly, in closed form, for the exciton systems that can be described by the hydrogenic (Wannier) approximation.

In Sec. IV we consider the zero-LO-phonon line. We calculate the acoustic-phonon-assisted optical spectrum using the Green's-function approach discussed in Sec. II, since the conventional perturbation theoretic formulation is inadequate for these processes. Both the piezoelectric and deformation potential coupling of the excitons to the acoustic phonons are considered. The results are related to the information obtained from observed spectra, and conclusions regarding the various approximations are discussed.

We conclude with Sec. V in which we compare the calculations based on the approach discussed in Sec. III with the reported LO-phonon-assisted emission. Line shapes and widths as well as the relative intensity of the one- to two-phonon peaks will be discussed. The contribution of other effects such as those due to the finite exciton lifetime and polariton effects will be considered.

II. GREEN'S-FUNCTION THEORY

The intrinsic optical absorption or emission of many nonmetals is best understood in terms of exciton states. By equating the emission or absorption of a photon with the simultaneous destruction or creation of an exciton state, the Coulomb interaction between the electron and hole is included properly. In good crystals and with the neglect of possible surface effects, the important mechanisms that cause line broadening and make possible true absorption and emission involving excitons are the interactions of the excitons with the lattice vibrations. In polar semiconductors it has been shown that the optical absorption below the exciton absorption peaks is associated with the simultaneous absorption of LO phonons and photons.² The related phonon-assisted emission will be discussed in the following sections. Thus, it is useful to have a general theory of optical

transitions incorporating exciton-phonon interactions. The most detailed study of the problem in the weak exciton-photon coupling approximation so far was by Toyozawa,¹⁰ who explained the origin of the asymmetry in the Cu₂O exciton line. Toyozawa's result (1.1) will be derived using a Green's-function formalism. The results for the emission transition probability will be discussed at the end of this section.

The Hamiltonian for the system will be written as

$$\mathcal{H} = \mathcal{H}_0 + \mathcal{H}_{\text{ex-R}} + \mathcal{H}_{\text{ex-L}} \quad (2.1a)$$

with the unperturbed part \mathcal{H}_0 being the sum of the Hamiltonians for the uncoupled excitons, photons, and phonons, while the two other terms, $\mathcal{H}_{\text{ex-L}}$ and $\mathcal{H}_{\text{ex-R}}$, represent the interactions of the excitons with the lattice vibrations and radiation, respectively. We take $c_{\lambda\mathbf{k}}^\dagger$ to be the creation operator for excitons, $a_{\mathbf{q}}^\dagger$ for photons, and $\alpha_{\mathbf{k}}^\dagger$ for phonons. We treat the excitons as bosons, although classical Boltzmann statistics actually apply for the experiments of interest. In this notation the first two terms in (2.1a) are

$$\mathcal{H}_0 = \sum_{\lambda\mathbf{k}} \epsilon_{\lambda\mathbf{k}} c_{\lambda\mathbf{k}}^\dagger c_{\lambda\mathbf{k}} + \sum_{\mathbf{q}} \omega_{\mathbf{q}} a_{\mathbf{q}}^\dagger a_{\mathbf{q}} + \sum_{\mathbf{k}} \omega_{\mathbf{k}} \alpha_{\mathbf{k}}^\dagger \alpha_{\mathbf{k}}, \quad (2.1b)$$

$$\mathcal{H}_{\text{ex-R}} = \sum_{\lambda\mathbf{k}} \frac{M_\lambda(\mathbf{K})}{\sqrt{\omega_{\mathbf{K}}}} [c_{\lambda\mathbf{k}}^\dagger \alpha_{\mathbf{K}} + \alpha_{\mathbf{K}}^\dagger c_{\lambda\mathbf{k}}]. \quad (2.1c)$$

In the explicit calculations of the phonon-assisted processes in Secs. III and IV, $\mathcal{H}_{\text{ex-L}}$ is taken to be linear in the phonon operators

$$\mathcal{H}_{\text{ex-L}} = \sum_{\lambda, \lambda'; \mathbf{K}, \mathbf{q}} V(\mathbf{q})_{\lambda\lambda'} c_{\lambda, \mathbf{K}+\mathbf{q}}^\dagger c_{\lambda', \mathbf{K}} (a_{\mathbf{q}} + a_{\mathbf{q}}^\dagger). \quad (2.1d)$$

This interaction, which is the one employed in almost all calculations (e.g., it is used in Toyozawa's¹⁰ and Suna's¹¹ papers), is appropriate for the cases considered below including the 2-LO processes.^{12,13} However, when one attempts to include higher-order effects and multiphonon processes in a realistic calculation, it is reasonable to inquire about possible comparable contributions from nonlinear terms in the interaction. Unfortunately, very little is known about the magnitude of these terms, and they are generally neglected. We note here that all results obtained in this section are general in this regard and do *not* depend on the linear interaction (2.1d).

It is convenient to assume that the matrix elements M_λ and $V_{\lambda\lambda'}$ are real. The optical-absorption coefficient can be evaluated by finding the rate of change of the photon number operator $N_{\mathbf{k}} = \alpha_{\mathbf{k}}^\dagger \alpha_{\mathbf{k}}$ (which has eigenvalues $n_{\mathbf{k}}$).

$$\partial N_{\mathbf{k}} / \partial t = i[\mathcal{H}, N_{\mathbf{k}}] = i[\mathcal{H}_{\text{ex-R}}, N_{\mathbf{k}}]. \quad (2.2)$$

Our aim is to evaluate the thermal average of (2.2) to order M^2 , while retaining terms in all powers of $V_{\lambda\lambda'}$.

¹¹ A. Suna, Phys. Rev. **135**, A111 (1964).

¹² B. Segall, Phys. Rev. **150**, 734 (1966).

¹³ See Sec. V of Ref. 12.

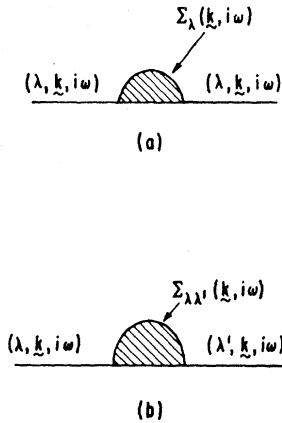


FIG. 2. Exciton self-energy diagrams. The self-energies $\Sigma_\lambda(\mathbf{K}, i\omega_n)$ and $\Sigma_{\lambda\lambda'}(\mathbf{K}, i\omega_n)$ with $\lambda \neq \lambda'$ are represented in (a) and (b), respectively.

In order to calculate this linear response, we want

$$\left\langle \frac{\partial N_{\mathbf{K}}}{\partial t} \right\rangle = -i \int_{-\infty}^t dt' \left\langle \left[\frac{\partial N_{\mathbf{K}}(t)}{\partial t}, \mathcal{H}_{\text{ex-R}}(t') \right] \right\rangle. \quad (2.3)$$

The rate of optical absorption is determined by the proportionality constant between $\langle \partial N_{\mathbf{K}} / \partial t \rangle$ and $n_{\mathbf{K}}$. From (2.3) and (2.1c) and with $\omega_{\mathbf{K}} = \omega$, we find

$$\begin{aligned} \left\langle \frac{\partial N_{\mathbf{K}}}{\partial t} \right\rangle &= \frac{n_{\mathbf{K}}}{\omega} \sum_{\lambda\lambda'} M_\lambda(\mathbf{K}) M_{\lambda'}(\mathbf{K}) \int_{-\infty}^t dt' \\ &\times \{ e^{-i\omega(t-t')} \langle [c_{\lambda\mathbf{K}}^\dagger(t), c_{\lambda'\mathbf{K}}(t')] \rangle \\ &- e^{i\omega(t-t')} \langle [c_{\lambda\mathbf{K}}(t), c_{\lambda'\mathbf{K}}^\dagger(t')] \rangle \}. \quad (2.4) \end{aligned}$$

Now let us define the retarded Green's function¹⁴

$$G_{\lambda\lambda'}^{\text{ret}}(\mathbf{K}, t-t') = -i\theta(t-t') \langle [c_{\lambda\mathbf{K}}(t), c_{\lambda'\mathbf{K}}^\dagger(t')] \rangle.$$

One can also define its Fourier transform $G_{\lambda\lambda'}^{\text{ret}}(\mathbf{K}, \omega)$. For optical absorption, we can set $\mathbf{K} = 0$, and $M_\lambda(0) = M_\lambda$. To within a constant, the absorption from (2.4) is given by

$$\omega W_{\text{abs}}(\omega) = -2 \sum_{\lambda\lambda'} M_\lambda M_{\lambda'} \text{Im} G_{\lambda\lambda'}^{\text{ret}}(0, \omega). \quad (2.5)$$

The optical absorption is obtained by evaluating the retarded function $G_{\lambda\lambda'}^{\text{ret}}$. This is not a conventional Green's function since we have not restricted the indices to $\lambda = \lambda'$. Let us define the equivalent Matsubara function

$$\mathcal{G}_{\lambda\lambda'}(\mathbf{K}, i\omega_n) = \int_0^\beta dt e^{i\omega_n(t-t')} \langle T_i c_{\lambda\mathbf{K}}(t) c_{\lambda'\mathbf{K}}^\dagger(t') \rangle.$$

This becomes a conventional Green's function $\mathcal{G}_\lambda(\mathbf{K}, i\omega_n)$ when $\lambda = \lambda'$. The function $\mathcal{G}_\lambda(\mathbf{K}, i\omega_n)$ can be obtained from Dyson's equation

$$\mathcal{G}_\lambda(\mathbf{K}, i\omega_n) = [i\omega_n - E_{\lambda, \mathbf{K}} - \Sigma_\lambda(\mathbf{K}, i\omega_n)]^{-1}.$$

¹⁴ A. A. Abrikosov, L. P. Gorkov, and I. E. Dzyaloshinski, *Methods of Quantum Field Theory in Statistical Mechanics* (Prentice-Hall, Inc., Englewood Cliffs, N. J., 1963).

The self-energy $\Sigma_\lambda(\mathbf{K}, i\omega_n)$ is the sum of all diagrams in which an exciton of (λ, \mathbf{K}) has virtual interactions and ends up again in $(\lambda, \mathbf{K}, i\omega)$. The state (λ, \mathbf{K}) cannot be an intermediate state. This definition is indicated schematically in Fig. 2(a). In the same way, we can define a self-energy $\Sigma_{\lambda\lambda'}(\mathbf{K}, i\omega_n)$ in terms of diagrams in which the exciton starts in $(\lambda, \mathbf{K}, i\omega)$ and ends in $(\lambda', \mathbf{K}, i\omega)$ and neither of these is an allowed intermediate state. This definition is shown in Fig. 2(b). In terms of this generalized self-energy, one can show by an examination of the diagrams for the Green's functions that

$$\begin{aligned} \mathcal{G}_{\lambda\lambda'}(\mathbf{K}, i\omega_n) &= \mathcal{G}_\lambda(\mathbf{K}, i\omega_n), & \lambda = \lambda' \\ &= \mathcal{G}_\lambda(\mathbf{K}, i\omega_n) \Sigma_{\lambda\lambda'}(\mathbf{K}, i\omega_n) \mathcal{G}_{\lambda'}(\mathbf{K}, i\omega_n), & \lambda \neq \lambda'. \end{aligned}$$

The retarded function $G_{\lambda\lambda'}^{\text{ret}}(\mathbf{K}, \omega)$ is obtained by letting $i\omega_n \rightarrow \omega + i\delta$. Let us define in the standard way

$$\begin{aligned} G_\lambda^{\text{ret}}(0, \omega) &= \text{Re} G_\lambda(\omega) - \frac{1}{2} i A_\lambda(\omega), \\ \Sigma_{\lambda\lambda'}^{\text{ret}}(0, \omega) &= \text{Re} \Sigma_{\lambda\lambda'}(\omega) + i \text{Im} \Sigma_{\lambda\lambda'}(\omega). \end{aligned}$$

Using (2.5), this gives our results for the absorption coefficient

$$\begin{aligned} \omega W_{\text{abs}}(\omega) &= \sum_\lambda |M_\lambda|^2 A_\lambda(\omega) + 2 \sum_{\lambda \neq \lambda'} M_\lambda M_{\lambda'} \\ &\times \{ \text{Re} \Sigma_{\lambda\lambda'}(\omega) A_\lambda(\omega) \text{Re} G_{\lambda'}(\omega) - \text{Im} \Sigma_{\lambda\lambda'}(\omega) \\ &\times [\text{Re} G_\lambda(\omega) \text{Re} G_{\lambda'}(\omega) - \frac{1}{4} A_\lambda(\omega) A_{\lambda'}(\omega)] \}. \quad (2.6) \end{aligned}$$

Suna¹¹ considered a model with just one λ state, so his result was just the first term of (2.6).

To relate the expression (2.6) to Toyozawa's result, (1.3), we consider the appropriate condition in which the exciton levels are distinctly separated. For energies near a particular line [i.e., $\omega \approx \tilde{\epsilon}_\lambda = \epsilon_{\lambda, 0} + \text{Re} \Sigma_\lambda(0, \omega)$], one can assume that $A_\lambda(\omega)$ and $\text{Re} G_\lambda(\omega)$ are the only functions which vary rapidly with ω . Then (2.6) can be recast into an equation of the form (1.3) with the func-

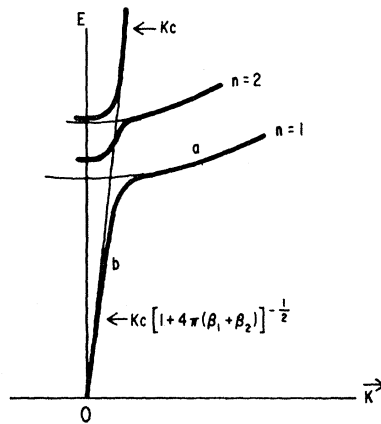


FIG. 3. Dispersion curve for "polaritons" associated with a hypothetical system containing two exciton bands. The lighter curves represent the dispersion curves for the unperturbed photon and exciton, while the heavier curves denote those for the eigenmodes of the interacting system—the polaritons.

tions $A_{\lambda'}$ and $\text{Re}G_{\lambda'}$, with $\lambda' \neq \lambda$, contributing to \tilde{C}_{λ} and to the renormalization of M . Specifically, we have

$$|\tilde{M}_{\lambda}|^2 \tilde{C}_{\lambda}(\omega) = - \sum_{\lambda' (\neq \lambda)} M_{\lambda} M_{\lambda'} \times \text{Im} \Sigma_{\lambda\lambda'}(\omega) \text{Re} G_{\lambda'}(\omega). \quad (2.7)$$

It is of some interest to see how the general expression (2.6) reduces in the weak-coupling limit to the conventional perturbation-theory result, for example, for the LO-phonon-assisted optical transition rate [Eq. (3.3)]. This is done in Appendix A. The resulting formula is the same as the perturbation-theory result, except that the effect of damping is included (i.e., the energy denominator $(\omega - \epsilon_{\lambda,0})^{-1} \rightarrow (\omega - \epsilon_{\lambda}) [(\omega - \epsilon_{\lambda})^2 + (\text{Im} \Sigma_{\lambda})^2]^{-1}$).

In order to calculate emission spectra, it is necessary to assume some distribution for the initial exciton states produced by the source of excitation. The most natural assumption to make, particularly in the weak-coupling approximation, is that the excitons are distributed above the bottom of the uncoupled exciton band according to a quasithermal equilibrium distribution. However, this assumption has been questioned by Hopfield.¹⁵ He notes, for example, that an initial excitonlike state such as indicated by the point a on the lowest-polariton band in Fig. 3 could move down the dispersion curve by the emission of many phonons eventually reaching a photonlike state (e.g., the point b) with energy well below $E_x(0)$. If this were an important process, the excitons would not "thermalize" above the "bottom" of the exciton band. On the other hand, we noted in Sec. I that a qualitative study of the emission data suggests that the excitons are populated according to a Boltzmann distribution and the results of the present calculations based on this distribution tend to confirm that view. That this is so probably results from the fact, pointed out by Toyozawa,¹⁶ that the knee of a polariton dispersion curve is a "bottleneck." That is, in that region, both the scattering time and the time it takes for a photon to "leak out" of the crystal are very long compared with the scattering time above the knee. It seems likely that if there are any appreciable deviations from the Boltzmann distribution, they would occur principally around the "knee." This would have its most pronounced effect on the zero-LO emission at low temperatures.

With the quasithermal distribution, it can be shown that the transition probabilities for emission and absorption are related by

$$W_{\text{em}}(\omega) \propto e^{-\omega/k_B T} W_{\text{abs}}(\omega), \quad (2.8)$$

which is equivalent to a statement of detailed balance.¹¹ In the work below, we first calculate the absorption as-

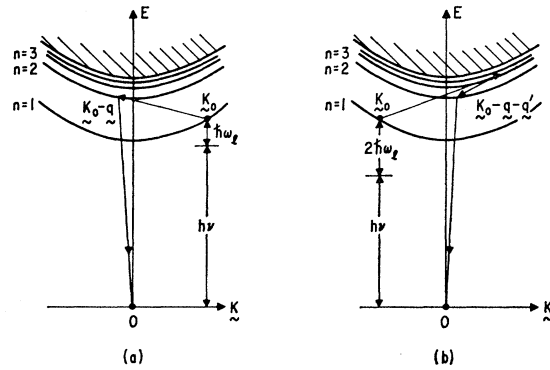


FIG. 4. Perturbation-theory representation of the LO-phonon-assisted optical absorption (emission) by the creation (annihilation) of "direct" excitons. The parabolas indicate the unperturbed "hydrogenic" exciton bands, the hatched area the bands in the continuum, and the dot at $E = \mathbf{K} = 0$ the ground state of the crystal. The scattering due to the emission (absorption) of the LO phonons is denoted by the lines between states of the exciton bands. The arrows are appropriate for the emission process. The drawing to the left represents the one-LO processes and the one to the right the two-LO processes.

suming that no thermal excitons are present and then find emission from Eq. (2.8).

III. LO-PHONON-ASSISTED EMISSION

A. Description of the Process

For the compound semiconductors of interest in this work, coupling to the lattice can be taken to be relatively weak. This is indicated by the fact that the "polaron" coupling constant α for these materials is less than unity. Furthermore, the coupling to the exciton is decidedly weaker than to a single carrier (the "polaron") because of the exciton's charge neutrality. A discussion of the justification and limitations of the use of the weak-coupling approximation for the interaction with the radiation will be given below.

The perturbation description for the optical processes, which has been given several times before,^{12,17} is represented in Fig. 4 for the one- and two-phonon processes. The parabolas denote the exciton bands, and the dot at $E = \mathbf{K} = 0$ represents the ground state of the system.¹⁸ We consider the one-phonon process which for optical absorption (fluorescence) proceeds with the annihilation (emission) of a phonon. We will be concerned with low temperatures [$T < (E_{x,2} - E_{x,1})/k_B \approx 275^\circ\text{K}$ for CdS], so the initial state for emission will be in the $n=1$ band. Correspondingly, we will restrict consideration to the $n=1$ final-state bands for the absorption. The process for absorption is described by two steps. The first is the excitation of the system by the annihilation of the photon of momentum $\hbar\mathbf{k}$ into the intermediate state in band n' with $\mathbf{K}' = \mathbf{k} \approx 0$. In the second step, the exciton

¹⁵ J. J. Hopfield, in *Proceedings of the International Conference on II-VI Semiconducting Compounds*, Providence, R. I. (W. A. Benjamin, Inc., New York, 1967), p. 786.

¹⁶ Y. Toyozawa, *Progr. Theoret. Phys. (Kyoto) Suppl.* **12**, 111 (1959).

¹⁷ D. G. Thomas, J. J. Hopfield, and M. Power, *Phys. Rev.* **119**, 570 (1960).

¹⁸ $E_{x,n}/k_B T$ is sufficiently large that the number of thermally excited excitons is completely negligible.

is scattered into the state $\mathbf{K}=\mathbf{q}+\mathbf{k}\approx\mathbf{q}$ with the annihilation of the phonon \mathbf{q} . In the fluorescence process, the two steps are essentially reversed. The initial state is an exciton in the state \mathbf{K} in the $n=1$ band, and it is scattered by the emission of an LO phonon into the intermediate state $\mathbf{K}'=\mathbf{k}\approx\mathbf{0}$ in the n' band. Emission of the photon \mathbf{k} takes the system to the ground state $E=\mathbf{K}=\mathbf{0}$. The two-phonon processes, which are illustrated in Fig. 4(b), are the direct extensions of the one-phonon processes.

We briefly consider the phonon-assisted emission process from the standpoint in which the exciton-photon interaction is treated accurately. In this case, the one-phonon emission consists of the scattering of a polariton^{9,19} from a state above the region of strong interaction, say, the one denoted by a in Fig. 3, to a state below this region, e.g., the point b where the polariton is essentially a photon. The coupling to the LO phonon is through the exciton component of the polariton. The perturbation theoretic result can be seen to agree with the result of this more accurate approach as long as the initial and final polariton states are not in the region in which there is strong mixing of the exciton and photon modes. Actually, appreciable differences occur only when the final (initial) polariton state in emission (absorption) has an energy which is close to $E_{x1}(0)$, i.e., when the energy denominators of perturbation theory become small.²⁰ From this we see that no significant errors would be expected for the two-LO process. Discrepancies can occur on the high-energy side of the one-LO emission peak for a certain range of temperature depending on the coupling parameter $4\pi\beta/\epsilon'$, $\hbar\omega_1$, and the breadth of the exciton states due to their interactions with phonons. On the other hand, it is clear from the above discussion that for the acoustic-phonon-assisted processes connected with the direct exciton, or zero-LO line, the polariton effects can be large. This is because both the initial and final states are in the region of strong interaction. In the work below we use weak coupling in $H_{\text{ex-R}}$.

As noted earlier, the absorption and emission are related by (2.8). For the conditions of interest, the absorption coefficient α_m for the simultaneous absorption of a photon and m -LO phonons is given by

$$\alpha_m(\omega) \propto W_{\text{abs}}^{(m)}(\omega) = N(\omega_1)^m |\mathfrak{M}_m(\omega)|^2, \quad (3.1)$$

where

$$N(\omega_1) = (e^{\beta\omega_1} - 1)^{-1}.$$

The factor $|\mathfrak{M}_m|^2$ is essentially the square of the overall matrix element. Using $N(\omega_1) = (1+N)e^{-\beta\omega_1}$ and setting $\hbar\omega_0$ in (2.8) equal to E_{x1} , the bottom of the $n=1$

exciton band, the detailed balance relation yields

$$W_{\text{em}}^{(m)}(\omega) \propto (1+N)^m e^{-\beta\Delta_m} |\mathfrak{M}_m(\omega)|^2. \quad (3.2)$$

This expression has the form expected for the emission process of interest according to the corresponding perturbation-theory approximation with the exponential reflecting the quasiequilibrium distribution of the excitons. Furthermore, it can be shown by an examination of the matrix elements, that the $\mathfrak{M}_m(\omega)$ which appears in (3.1) is precisely the factor that perturbation theory would yield for the emission process involved.

B. Sum Over Intermediate States for the One-LO Process

According to perturbation theory, the optical-absorption probability per photon for one-LO-phonon-assisted transitions to the $n=1$ exciton state is

$$\omega W_{\text{abs}}(\omega) = \frac{2\pi}{\hbar} N \Gamma \gamma_0 \int \frac{d^3q}{(2\pi)^3} \mathcal{U}_0(\mathbf{q}) \times \left| \sum_{\lambda} \frac{\psi_{\lambda}(0) \mathcal{U}_{\lambda,1S}(\mathbf{q})}{\epsilon_{\lambda,0} - \hbar\omega} \right|^2 \delta(\epsilon(\mathbf{q}) - \Delta_1), \quad (3.3)$$

where

$$\gamma_0 = \pi\beta_1/\epsilon' |\psi_{1S}(0)|^2,$$

$$\mathcal{U}_0(\mathbf{q}) = 4\pi\alpha_p(\hbar\omega_1)^{3/2} q^{-2} (2m)^{-1/2} \hbar = 2\pi(\epsilon_{\infty}^{-1} - \epsilon_S^{-1}) e^2 \hbar\omega_1/q^2, \quad (3.4)$$

$$\epsilon(\mathbf{q}) = \hbar^2 q_1^2/2M_1 + \hbar^2 q_{11}^2/2M_{11},$$

$$\mathcal{U}_{\lambda,1S}(\mathbf{q}) = \int d^3r \psi_{\lambda}^*(\mathbf{r}) [e^{i\mathbf{Q}_e \cdot \mathbf{r}} - e^{i\mathbf{Q}_h \cdot \mathbf{r}}] \psi_{1S}(\mathbf{r}), \quad (3.5)$$

$$\mathbf{Q}_e = m_e/M_1(q_x, q_y, q_z [m_{h1}M_1/m_{11}M_{11}]^{1/2}), \quad (3.6)$$

$$\mathbf{Q}_h = -m_{h1}/M_1(q_x, q_y, q_z [m_{h1}M_1/m_{h1}M_{11}]^{1/2}),$$

and $4\pi\beta_1$ is the contribution of the $n=1$ exciton band to the low-frequency polarizability. The vectors \mathbf{Q}_e and \mathbf{Q}_h result from the combination of a transformation from \mathbf{r}_e and \mathbf{r}_h to relative and center-of-mass coordinates and a certain transformation on the relative coordinates for wurtzite crystals. In these crystals, the valence bands are quite anisotropic and, consequently, the exciton wave functions are relatively complicated. In the transformed (relative) coordinate system the wave functions are "hydrogenic" to an accuracy sufficient for our purposes.²¹ The anisotropy does produce a quantitatively important effect in the absorption and emission, and we take it into account in our calculations.

The matrix element in (3.3) contains the sum over λ , which means that the phonon can scatter the exciton into different exciton bands. In this section we show that one can evaluate the sum exactly when the spectrum and eigenfunctions are hydrogenic.

²¹ B. Segall, Phys. Rev. 163, 769 (1967).

¹⁹ W. C. Tait, D. A. Campbell, J. R. Packard, and R. L. Weiher, in *Proceeding of the International Conference on II-VI Semiconducting Compounds*, Providence, R. I. (W. A. Benjamin, Inc., New York, 1967), p. 370.

²⁰ The relevant energy difference appears to be $(4\pi\beta/\epsilon')^{1/2} E_{x1}$, which is typically a few one hundredths of an eV for the II-VI compounds.

The sum we are concerned with is

$$S(\mathbf{q}, \Delta) = S_e(\mathbf{q}, \Delta) - S_h(\mathbf{q}, \Delta) = \sum_{\lambda} \frac{\psi_{\lambda}(0) \mathcal{U}_{\lambda,1S}(\mathbf{q})}{\epsilon_{\lambda,0} - \Omega - E_G}$$

or

$$S_e(\mathbf{q}, \Delta) = \int d^3r \left\{ \sum_{\lambda} \frac{\psi_{\lambda}(0) \psi_{\lambda}^*(\mathbf{r})}{\epsilon_{\lambda,0} - \Omega - E_G} \right\} e^{i\mathbf{Q} \cdot \mathbf{r}} \psi_{1S}(\mathbf{r}), \quad (3.7)$$

where

$$\Omega = \Delta - B - \omega_l.$$

From the eigenfunction expansion for the Green's function,

$$G(\mathbf{r}, \mathbf{r}'; \Omega) = - \sum_{\lambda} \frac{\psi_{\lambda}(\mathbf{r}) \psi_{\lambda}^*(\mathbf{r}')}{\epsilon_{\lambda,0} - \Omega - E_G},$$

it is seen that we require only $G(0, \mathbf{r}'; \Omega)$ to evaluate (3.7). Fortunately, this function can be expressed in a reasonably tractable form for the case that ψ_{λ} and $\epsilon_{\lambda,0}$ are hydrogenic. The required function is²²

$$G(0, \mathbf{r}; \Omega) = -\mu(2\pi r)^{-1} \Gamma(1-\nu) W_{\nu, 1/2}(2r/av),$$

where $\Gamma(Z)$ and $W(Z)$ are the gamma and second Whittaker functions, respectively,

$$\nu = [B/(B + \omega_l + \Delta)]^{1/2},$$

μ is the reduced mass, and B the exciton binding energy. We find

$$S_e(\mathbf{q}, \Delta) = 2\mu Q^{-1} \psi_{1S}(0) \Gamma(1-\nu) \int_0^{\infty} dr \times e^{-r/a} \sin(Qr) W_{\nu, 1/2}(2r/av). \quad (3.8)$$

The integral in (3.8) is a complex Laplace transform of the Whittaker function, and it can be obtained from the tabulated integral²³

$$\int_0^{\infty} e^{-px} x^{\nu-1} W_{\sigma, \mu}(ax) dx = \frac{\Gamma(\mu + \eta + \frac{1}{2}) \Gamma(\eta + \frac{1}{2} - \mu) a^{\mu+1/2}}{\Gamma(\eta + 1 - \sigma) (a/2 + p)^{\mu+\eta+1/2}} \times {}_2F_1\left(\mu + \eta + \frac{1}{2}, \mu + \frac{1}{2} - \sigma; \eta + 1 - \sigma; \frac{2p-a}{2p+a}\right),$$

with ${}_2F_1$ the hypergeometric function. With the use of the standard transformation on hypergeometric functions,

$$F(a, b; c; z) = (1-z)^{-a} F[a, c-b; c; z/(z-1)],$$

S_e can be expressed in the relatively simple form

$$S_e(\mathbf{q}, \Delta) = \frac{\psi_{n=1}(0)\nu}{2aBQ_e(1-\nu)} \times \text{Im} {}_2F_1(2, 1; 2-\nu; \frac{1}{2}[1-\nu(1-iQ_e a)]). \quad (3.9)$$

$S_h(\mathbf{q}, \omega)$ is obtained by replacing \mathbf{Q}_e with \mathbf{Q}_h .

²² L. Hostler, J. Math. Phys. 5, 591 (1964).

²³ Tables of Integral Transforms, edited by A. Erdelyi (McGraw-Hill Book Co., New York, 1954), Vol. 1, p. 216.

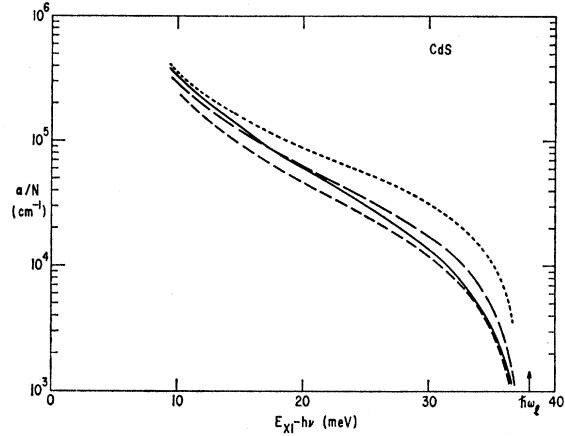


FIG. 5. One-LO-phonon-assisted CdS optical-absorption coefficient calculated with the exact and approximate summation over intermediate states. The results are for an isotropic valence band with a mass $m_h = (m_{h1}^2 m_{h11})^{1/3}$. The solid curve is the result which accurately includes all intermediate bands. The dotted curve is that in which only the $n=1$ intermediate band is included. The results obtained by using the "average excitation" approximation with $(\langle E_{x1} \rangle - E_{x1})B^{-1} = 2$ and 4 are given by the short and long dashed curves.

Let us first consider the case of isotropic exciton bands ($m_{h1} = m_{h11} = m_h$, $M_1 = M_{11} = M$), which are relevant for nondegenerate electronic bands in the cubic materials. Then

$$\mathbf{Q}_e = (m_e/M)\mathbf{q}, \quad \mathbf{Q}_h = -(m_h/M)\mathbf{q}.$$

The magnitude of \mathbf{q} , the momentum of the phonon, is fixed by energy conservation, $\Delta = q^2/2M$. The absorption coefficient is obtained from the absolute square of $S(\omega)$ as described earlier [e.g., Eq. (12) of Ref. 12] and for $n_f = 1$ is given by

$$\alpha(\hbar\omega) = \frac{\pi\beta_1\alpha_p(\hbar\omega_1)^{3/2}\mu M}{2(\sqrt{\epsilon'})c\hbar B(\Delta_1)^{3/2}} \left(\frac{\nu}{1-\nu}\right)^2 \times |m_e^{-1} \text{Im} F_e - m_h^{-1} \text{Im} F_h|^2, \quad (3.10)$$

where $\text{Im} F$ denotes the imaginary part of the hypergeometric function in (3.9). This exact result (for the perturbation approximation and hydrogenic exciton systems) is gratifyingly simple.

It is interesting to compare the above result with the results of previous approximations. This is done in Fig. 5 using parameters appropriate to CdS except that the hole mass tensor is replaced by an isotropic mass $m_h = (m_{h1}^2 m_{h11})^{1/3}$. The cruder of the two approximations involved the neglect of all intermediate states except the $\lambda = n = 1$ state.¹⁷ This approximate result is about a factor of 3 too large in the region just above the threshold. In the other procedure, the sum was treated by evaluating the first few (three) terms exactly, replacing the energy denominator $\epsilon_{\lambda} - \omega = E_{x\lambda} - \omega$ by $\langle E_{x\lambda} \rangle - \omega$ and summing the remaining terms by the use of the closure relation.¹² It is seen from Fig. 5 that for reasonable values of the "average excitation" $\langle E_{x\lambda} \rangle$

$-E_{x1}$ of 2 to $4B$, these approximate results represent a significant improvement over the simplest approximation, particularly near threshold. The differences between these approximate results and the exact results are about 25% over some range of $\hbar\omega$ which depends on the value of the "average excitation."

The behavior of (3.10) above the threshold is

$$\alpha \sim q^3 \sim \Delta_1^{3/2}, \quad (3.11)$$

with Δ_1 given by (1.2). Because of the Boltzmann factor in the emission probability, excitons of low kinetic energy, or photons of energy slightly above the one-phonon threshold, are of most interest for fluorescence. Using Eqs. (2.8) and (3.11), the one-phonon emission probability $P_1(\hbar\omega)$ is

$$P_1 \sim \Delta_1^{3/2} e^{-\Delta_1/k_B T}. \quad (3.12)$$

Gross *et al.*⁴ suggested the spectral dependence (3.12) for the one-phonon emission on the basis of the approximate $\frac{3}{2}k_B$ value of the slope of the measured one-phonon widths versus temperature. The $\Delta^{3/2}$ threshold behavior in (3.12) arises from linear dependence of the scattering matrix element on Δ_1 at small Δ_1 (because of the neutrality of the exciton manifested by the cancellation between the electron and hole terms) and the $\Delta^{1/2}$ density-of-states factor. Above threshold (but still in a region of interest for moderate to high T) the actual behavior of $\alpha_{1ph}(\hbar\omega)$ is a much more rapidly increasing function of Δ_1 (see the calculations of α_{1ph}); but, of course, the importance of this behavior is somewhat suppressed by the Boltzmann factor.

From the magneto-optical exciton studies^{1,2} of the wurtzite compounds, particularly CdS, it is known that the conduction bands are nearly isotropic while the upper valence bands are rather anisotropic (e.g., for CdS $m_{h11}/m_{h1} \sim 5$). As stated earlier, the effect of these anisotropies on the relative motion is reasonably small and to a good approximation the scattering matrix elements are the same as those for the cubic case except that the more general \mathbf{Q}_e and \mathbf{Q}_h of (3.6) must be used. The effect on the center-of-mass motion on the other hand is appreciable with the exciton bands being quite anisotropic. In contrast to the cubic case where q is fixed by $\epsilon(\mathbf{q}) = \Delta$ and the sum over final states ($n=1$, $\mathbf{K}=\mathbf{q}$) in absorption is trivial, here there is a range of q satisfying energy conservation. Thus, in the anisotropic case, the sum over final states leads to an integral in the evaluation of (3.3). This integral is evaluated numerically.

C. Two-LO-Phonon-Assisted Process

It appears too impractical to compute the double sums of intermediate states exactly for the rather complicated two-phonon processes, which are third-order processes. In the two-LO-phonon results presented below, the contribution of the intermediate states will be included by an approximate method involving the

average excitation energy $\langle \epsilon_\lambda \rangle - \epsilon_{1S}$, and the use of closure.¹² For isotropic bands we will use the result derived for the cubic crystals, i.e., Eq. (25) of Ref. 12. As noted above, the threshold behavior is of interest. It is clear from a consideration of the kinematics and the general behavior of the scattering matrix elements that the only parts of phase space that contribute to the processes around the two-phonon threshold are those for $\mathbf{q}' \approx -\mathbf{q}$.

From Eqs. (23)–(25) of Ref. 12, it can be seen that around threshold the two-phonon contribution to the absorption is

$$\alpha_{2ph}(\hbar\omega) \sim \Delta_2^{1/2} \int_0^\infty q dq |\{\mathbf{q}; -\mathbf{q}\}|^2, \quad (3.13)$$

where

$$|\{\mathbf{q}; -\mathbf{q}\}|^2 \approx 4 \left\{ |\langle 1 | U(\mathbf{q}) | 1 \rangle|^2 \right. \\ \times \left[\frac{1}{\epsilon(\mathbf{q}) + \hbar\omega_l} - \frac{1}{\langle E_{xn} \rangle - E_{x1} + \epsilon(\mathbf{q}) + \hbar\omega_l} \right] \\ \left. + \langle 1 | U(\mathbf{q}) U(-\mathbf{q}) | 1 \rangle \frac{1}{\langle E_{xn} \rangle - E_{x1} + \epsilon(\mathbf{q}) + \hbar\omega_l} \right\}^2$$

is independent of $\hbar\omega$ (since all the energy denominators are nearly constant around $\hbar\omega = E_{x1} - 2\hbar\omega_l$). It follows that around threshold the two-LO-phonon-assisted emission probability is

$$P_2 \sim \Delta_2^{1/2} \exp(-\Delta_2/k_B T). \quad (3.14)$$

The expression for the two-phonon contribution to the absorption coefficient for the anisotropic case is too complex to permit feasible computation for general $\hbar\omega$. However, the expression simplifies considerably around the threshold and has the same energy dependence as (3.13). Also of interest is the dependence of α on the band anisotropy. It is shown in Appendix B that this dependence is given by $(M_1^2 M_{11})^{1/2}$ times a rather weakly varying function of the mass anisotropy, so that α_{2ph} is approximately proportional to a density-of-states mass factor. With the exception of this factor, then, we can with accuracy sufficient for our purpose use the expressions for α_{2ph} in Ref. 12 for wurtzite.

It is interesting to note that Gross *et al.*⁴ arrived at Eq. (3.14) for the two-phonon emission by arguing that the probability for the process can be factored into the Boltzmann factor and a probability, $W_2(\mathbf{K})$, that an exciton of momentum \mathbf{K} will create two LO phonons in scattering to $\mathbf{K} \approx 0$. The $W_2(\mathbf{K})$ is the sum of the probabilities for creating phonon pairs with allowable momenta (i.e., $\mathbf{q} + \mathbf{q}' = \mathbf{K}$). Furthermore they argued that the sum will include significant contributions from q and q' larger than K so that W_2 is essentially independent of \mathbf{K} (and $\hbar\omega$). As we can see from the above discussion of the perturbation-theory result, this is essentially correct around the *threshold*. Above threshold, the fact that

the states resulting from the scattering of the exciton are intermediate states of the over-all process becomes more important and the above approximation becomes less adequate. The photon energy dependence arising from the energy denominators is by no means negligible above threshold.

IV. ACOUSTIC-PHONON-ASSISTED EMISSION: ZERO-LO LINE

In this section we study by perturbation theory (in $\mathcal{H}_{\text{ex-R}}$) the direct emission, or the zero-LO phonon line, which in CdS at 4.2°K is at 4853 Å. The shape and breadth of this line and, indeed, the radiative decay itself in a perfect crystal, are due to interaction with acoustic phonons.⁹ This interaction leads to a finite linewidth $\Gamma(\epsilon) = -\text{Im}\Sigma(0, \epsilon)$, and if the width is essentially independent of ϵ , to a Lorentzian shape according to (1.3).

It is not possible to calculate the acoustic-phonon process by the standard "Golden rule" perturbation approach because of the occurrence of a divergence in the transition rate (and self-energy) at small exciton kinetic energy. To properly calculate this process in perturbation theory, it is necessary to use the Green's-function results derived in Sec. II. Since only phonons of small \mathbf{q} are involved, and since the $V_{\lambda\lambda'}(\mathbf{q})$ for $\lambda \neq \lambda'$ [see Eq. (A1)] are negligible in this case (owing to the orthogonality of the exciton wave functions), we can neglect all terms but the first on the right-hand side of (2.6). Furthermore, since $\omega \approx \tilde{\epsilon}_{1s}$, the emission probability reduces to

$$P(\Delta) = \gamma_0 \hbar^{-1} e^{-\Delta/k_B T} |\psi_{1s}(0)|^2 A_{1s}(\mathbf{K} \approx 0, \Delta), \quad (4.1)$$

with the spectral density A_{1s} given by

$$A_{1s}(\mathbf{K} \approx 0, \Delta) \equiv A(\Delta) = 2\Gamma(\Delta)/[\Delta^2 + \Gamma(\Delta)^2]. \quad (4.2)$$

In (4.2) we have assumed that $\text{Re}\Sigma_{1s}(0, \Delta)$ is essentially constant for $\Delta = \omega - \epsilon_{1s} \approx 0$. The energy dependence of Γ arises from the various scattering mechanisms

$$\Gamma = \Gamma_p + \Gamma_{dp} + \Gamma_0,$$

where Γ_p and Γ_{dp} correspond to contributions from the piezoelectric and deformation-potential interactions. The Γ_0 arises from the other mechanisms such as impurity scattering, but we neglect these in the following.

The acoustical-phonon contributions are

$$\Gamma_j(\Delta) = \hbar \int \frac{d^3q}{(2\pi)^3} |V_j(\mathbf{q})|^2 \left\{ N_q \delta\left(\Delta - \frac{q^2}{2M} + c_s q\right) + (N_q + 1) \delta\left(\Delta - \frac{q^2}{2M} - c_s q\right) \right\}, \quad (4.3)$$

where $V_j(\mathbf{q})$ ($j = p$ or dp) represents the piezoelectric or deformation-potential interactions and c_s the sound

velocity. The former, which results from electric fields produced by the displacements of the ions, interacts equally but with opposite sign on the electron and hole. The $V_p(\mathbf{q})$ is given by

$$|V_p(\mathbf{q})|^2 = 2\pi g \hbar^3 c_s^2 q^{-1} |\mathcal{U}_{\lambda,1s}(\mathbf{q})|^2, \quad (4.4)$$

where $\mathcal{U}_{\lambda,1s}(\mathbf{q})$ is defined by (3.5), and g is a parameter determining the strength of the piezoelectric interaction. At small q this vanishes like q^3 so that the coupling is very weak, reflecting the exciton's charge neutrality. On the other hand, the deformation-potential coupling acts with different strengths on electrons and holes so that in general there is no cancellation. At long wavelengths then, the exciton couples to the acoustic phonons predominantly through the deformation potential. For the conditions of interest the coupling is

$$|V_{dp}(\mathbf{q})|^2 = D_{\text{ex}}^2 \hbar q (2\rho c_s)^{-1} [1 + O(q^2 a^2)], \quad (4.5)$$

where D_{ex} is $D_e^{\text{LA}} + D_h^{\text{LA}}$ and D_h^{TA} for the LA and TA modes, respectively,^{24,25} and ρ is the density.

To evaluate (4.3), we note that for the important \mathbf{q} , N_q is large compared with unity. For convenience we define $\epsilon_s = \frac{1}{2} M c_s^2 \approx 10^{-5}$ eV, $x = q/2M$, and $F_j(x) = x^2 |V_j(x)|^2 N(x)$. The integrals readily yield

$$\Gamma_j(\Delta) = \frac{(2M)^{3/2} \theta(\Delta + \epsilon_s)}{\hbar^3 2\pi (\Delta + \epsilon_s)^{1/2}} [F_j(|\sqrt{\epsilon_s} - (\Delta + \epsilon_s)^{1/2}|) + F_j(\sqrt{\epsilon_s} + (\Delta + \epsilon_s)^{1/2})], \quad (4.6)$$

with $\theta(s) = 0$ for $s < 0$ and $\theta(s) = 1$ for $s > 0$. The function (4.6) diverges as $\Delta + \epsilon_s \rightarrow 0$, and while this would invalidate the "Golden rule" result, it causes no problem in the emission distribution (4.1) because of the Γ^2 in the denominator of the spectral function. Since $F_{dp} \sim x^2$, (4.6) has the following simple form for the deformation-potential interaction:

$$\Gamma_{dp}(\Delta) = \frac{(2M)^{5/2} D_{\text{ex}}^2 (\Delta + 2\epsilon_s) \hbar_B T}{8\pi \hbar^3 \rho \epsilon_s (\Delta + \epsilon_s)^{1/2}} \times \theta(\Delta + \epsilon_s) [1 + O(\Delta/B)]. \quad (4.7)$$

The corresponding expression for $\Gamma_p(\Delta)$ is easily obtained from (4.6) and $F_p(x) \sim x^4$; but it is much smaller, as noted earlier.

Spectral functions (4.2) were obtained using (4.7). In spite of the obvious asymmetry in (4.7), it was found that for realistic parameters, the line shape is rather Lorentzian in appearance and quite narrow. It appears to have an effective width $\Gamma(0) \approx 10^{-2} k_B T$. The measured widths at moderate to low temperature on the other

²⁴ The electrons interact only with the LA phonons. The holes also interact with the LA modes and in zinc blende even more strongly with the TA modes (Ref. 25). While the coupling of the holes to the TA phonons in wurtzite has not yet been carefully investigated, it is probably reasonably strong there, too.

²⁵ G. D. Mahan, J. Phys. Chem. Solids **26**, 751 (1965).

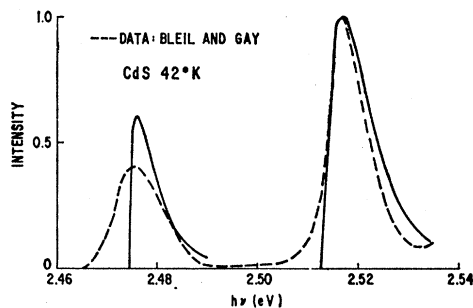


FIG. 6. Calculated one-LO- and two-LO-phonon-assisted fluorescence peaks (solid curve) for CdS at 42°K, compared with the spectrum (dashed curve) observed by Bleil and Gay.

hand are roughly about $k_B T$; these values are vastly larger than the calculated result. Since our approach is valid within the weak exciton-photon coupling framework, and since it is not clear how extrinsic effects (including surface effects) could explain the magnitude or temperature dependence of the observed linewidth, we conclude that the use of perturbation theory in regards $\mathcal{H}_{\text{ex-R}}$ is at fault.

It is not difficult to see why a low value is obtained. Energy and momentum conservation for the exciton in the *unperturbed* exciton band and the weak-coupling form [Eq. (4.2)] for the spectral function effectively restrict the range of exciton recoil momentum which contributes to the peak to very small values, which insures a small value for (4.3). With a considerably different dispersion relation for polaritons, this restriction is much less severe, so that much larger values can be achieved. The problem of acoustic-phonon-assisted emission in terms of polariton scattering has very recently been investigated by Tait and Weiher,²⁶ who obtain more reasonable values by this means.

Note added in proof. It should be noted, however, that Tait and Weiher used the value of 30 eV for the deformation potential to obtain their results. With this value of D_{ex} , which is a factor of ten larger than that used in our estimate, the perturbation theory result [Eq. (4.7)] also yields a $\Gamma_{\text{ep}}(0)$ of the order of $k_B T$. Although this result is in accord with the reported widths, we believe that the 30-eV value of D_{ex} is much too large. Recent stress experiments on CdS and other II-VI compounds [J. E. Rowe, M. Cardona, and F. H. Pollak, *Proceedings of the International Conference on II-VI Semiconducting Compounds, Providence, R. I.* (W. A. Benjamin, Inc., New York, 1967), p. 112; T. Koda and D. W. Langer, *Phys. Rev. Letters* **20**, 50 (1968)] have, in fact, shown that the deformation potentials are roughly 2 to 3 eV which is close to the value used in our estimate. It would appear then that a completely satisfactory calculation of the low-temperature linewidth has not yet been made. As noted above, the strong exciton-photon coupling must be taken into account in such a calculation.

²⁶ W. C. Tait and R. L. Weiher, *Phys. Rev.* **166**, 769 (1968).

V. COMPARISON WITH OBSERVED LO-PHONON-ASSISTED SPECTRA AND DISCUSSION

In this section we compare the emission spectra calculated by the methods described above. The relevant spectra have been studied far more extensively in CdS^{4,8,19,27} than in any other material, although there are some published data on ZnO⁶ and rather limited data on CdSe.⁶ As a result, we will concentrate largely on CdS. The first aspect to be considered will be the shapes of the peaks for which published spectra are available for just a few temperatures. Figure 6 shows the 42°K one-LO- and two-LO-assisted emission peaks in CdS observed by Bleil and Gay²⁷ along with the calculated spectra. Except for the use of the average excitation $\langle E_{\text{ex}} \rangle - E_{\text{ex}1} = 0.08$ eV ($\approx 3B$) for the two-LO-assisted emission, only experimentally determined parameters were employed in the calculations (given in Table I of Ref. 21). The intensity was normalized to the data at the peak of the higher-energy emission.

The calculated spectrum is in reasonable accord with the data, particularly for the one-LO peak. For the lower-energy peak the agreement is somewhat poorer, with the width of the observed peak significantly larger than that for the calculated result (and also that of Gross *et al.*⁴) and with the apparent threshold almost 5 meV below the calculated threshold.²⁸ The reasons for these discrepancies are not known with certainty. However, it seems plausible that a substantial part of the emission below the threshold is due to an overlapping extrinsic emission band. This view is consistent with the presence of an impurity emission band of appreciable intensity about 5 meV below the zero-LO free-exciton peak (see Fig. 2 of Ref. 27). The two-LO-assisted emission from this band will overlap the two-LO emission from the free excitons. These extrinsic emissions dominate the 4.2°K spectra. We note that Bleil and

TABLE I. Calculated and measured peak widths of the one-LO and two-LO phonon-assisted emission peaks.

T (°K)	One-LO		Two-LO	
	Calc. (eV)	Obs. (eV)	Calc. (eV)	Obs. (eV)
12	0.0034	0.003, ^a 0.004, ^b 0.006 ^c	0.0018	0.003, ^a 0.003, ^b 0.009 ^c
42	0.0097	0.011, ^a 0.009 ^c	0.0057	0.008, ^a 0.012 ^c
77	$\approx 0.015^d$	0.016 ^c 0.020, ^e	0.012	0.014 ^a 0.016 ^c 0.018 ^c

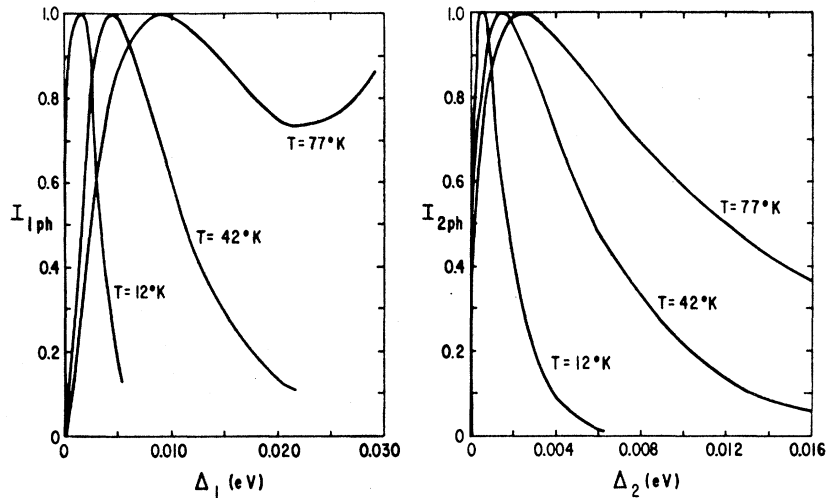
^a Reference 4.
^b Reference 19.
^c Reference 27.

^d Only rough estimate possible.
^e Reference 6.

²⁷ C. E. Bleil and J. G. Gay, in *Proceedings of the International Conference on II-VI Semiconducting Compounds, Providence, R. I.* (W. A. Benjamin, Inc., New York, 1967), p. 360.

²⁸ The calculated thresholds are obtained from $E_{\text{ex}1}(T)$ values interpolated from the exciton positions at various temperatures given by Thomas *et al.* in Ref. 17.

FIG. 7. Calculated one-LO- and two-LO-phonon-assisted emission peaks for CdS at $T=12, 42,$ and 77°K .



Gay have observed that the low-temperature widths of the phonon-assisted free-exciton peaks, and in particular the two-LO line spectrum, are quite large in their spectra. With this interpretation, it is seen that the calculated spectra are in quite reasonable accord with the measurements. We must note at this point that there is a fair variation in the details (i.e., the peak widths and shapes) of the various sets of CdS spectra that have been published to date. This, of course, complicates comparison with theory.²⁹

As the temperature rises the excitons are distributed to higher energies in the bands and, correspondingly, the final states in the polariton scattering picture move up in energy. At liquid-nitrogen temperatures it is found that for photon energies somewhat above the peak the final polariton states are already in the region where appreciable mixing occurs and where the perturbation-energy denominator is quite small. As noted earlier, under these circumstances the polariton effects must be taken into account. This has been done in the calculations of the one-LO peak in CdS at 77°K by Tait *et al.*¹⁹ who utilized Hopfield's polariton formalism. They note that the polariton aspect of the problem introduces a substantial effective linewidth $(4\pi\beta_1/\epsilon')^{1/2}E_{x1}$, which is larger than the widths due to the exciton-phonon interaction at 77°K or to impurity scattering. This prevents the energy-denominator factor from increasing drastically as $\hbar\omega \rightarrow E_{x1}$. At 77°K , for example, the emission intensity given by perturbation theory with $\Gamma_{1S} = \text{Im}\Sigma_{1S} = 0$ begins to rise again with in-

creasing energy for $\hbar\omega$ about 25 meV above the calculated threshold (i.e., about 15 meV above the position of the peak). This is illustrated in Fig. 7. Thus, above liquid-nitrogen temperature and until Γ_{1S} becomes appreciable, the polariton approach is required to obtain a good description of the emission on the high-energy side of the one-LO peak. It should be clear that the region over which these effects are important will depend on the parameters of the material, particularly $\hbar\omega_l$. For example, in ZnO, where $\hbar\omega_l$ is large, the emission is well removed from E_{x1} and, as we will see (Fig. 9), the perturbation theoretic treatment is completely adequate for the one-LO (and, of course, the two-LO) emission.

It was noted in Sec. III A that while the one-LO assisted processes are second-order in perturbation theory, they are of first order in the polariton treatment. It might seem then that only a single exciton band is involved. This is not the case. In the region where the exciton photon coupling is strong, all of the allowed exciton bands are admixed in the polariton bands. In fact, it can readily be shown that under the condition of interest (i.e., $\hbar\omega \approx E_{x1} \gg B$) the relative amplitude of the uncoupled exciton band n mixed in the lowest polariton band is given quite accurately by

$$E_{xn}(4\pi\beta_n)^{1/2}/[E_{x,n} - \hbar\omega(\mathbf{k})],$$

where $\hbar\omega(\mathbf{k})$ is the polariton energy. Except for the effect of the polariton dispersion for $n=1$ when $\hbar\omega(\mathbf{k})$ is on the lowest branch, this factor is essentially identical to the one appearing in the perturbation-theory expression [see Eq. (3.3)]. Since the inclusion of $n>1$ intermediate-state bands has been shown to lead to quantitatively significant corrections in the perturbation calculations (see Sec. III B), it can be expected to be significant in the polariton treatment as well. As yet, it has not been taken into account in those calculations.¹⁹

Calculated line shapes for a number of temperatures are given in Fig. 7. The calculated peaks all have the

²⁹ Comparison with the data of Gross *et al.* at this temperature (Fig. 1) is more difficult for two reasons. First, there is a considerably larger "background" from emissions associated with defects. Secondly, for some unknown reason both the peaks and the thresholds of the one-LO and two-LO emissions appear to lie about 7 meV lower than the values calculated from the position of the zero-LO exciton peak that they reported for that temperature. That these low values of the threshold are probably not real is also indicated by the differences with respect to the measurements of Bleil and Gay at 42°K and with the fact that there are no discrepancies between the calculated and measured thresholds for the 12°K data of Tait *et al.* (Ref. 19) and 77°K data of Packard *et al.* (Ref. 6).

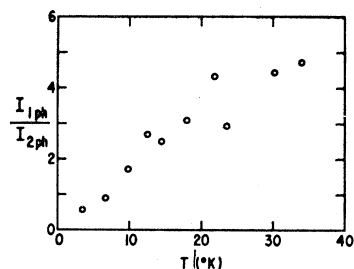


FIG. 8. The measured intensity ratio of one-LO- and two-LO-phonon-assisted emission peaks from the data of Gross *et al.*

expected nearly Maxwellian shape (except the 77°K one-LO peak which has a second rising portion as discussed above). It is seen that the one-LO peak tends to be slightly broader than the two-LO emission. This results from the fact that α_{1ph} is a more rapidly varying function of Δ_1 than α_{2ph} is of Δ_2 .

The widths corresponding to emission shown in Fig. 7 are given in Table I along with those obtained from the measurements.³⁰ Differences in the widths reported by different groups are evident. The 12° and 42°K widths of Bleil and Gay,²⁷ particularly for the two-LO peak, are larger than the other listed values, probably for the reason given earlier. The calculated values are seen to be in reasonably good accord with the measured values. It is noteworthy that the calculated values are always smaller than the data. Aside from the scatter in the measured values and questions about possible contributions from defect-associated emissions, two other factors must be considered in regard to this comparison. These are that both the inclusion of polariton effects and the finite values of Γ_λ would lead to an increase in the breadth of calculated emission. The first was discussed above. The latter could be important at both low temperatures (e.g., $T < 20^\circ\text{K}$), where the breadth due to the LO assistance is so small that a modest broadening of the order of 1 to 2 meV (due to acoustic phonons, imperfections, or random strains) would be significant, and at moderate to high temperature ($T > 70^\circ\text{K}$) where the thermal broadening of the exciton band becomes appreciable. It has been shown in other II-VI compounds that this broadening is a consequence of the reduction of the exciton lifetime due to the absorption of LO phonons.³¹ Bleil and Gay²⁷ have clearly shown that the temperature dependence of the widths of the one-LO and two-LO, as well as the zero-LO peaks in CdS exhibit a break at about 65°K due to a contribution which behaves as $[\exp(\hbar\omega_1/k_B T) - 1]^{-1}$. Gutsche and Voigt³² have also found this dependence in

³⁰ The calculated widths of the two-LO peaks reported here are about 25% larger than those tabulated in Ref. 5. This was due to the inadvertent omission in the previous computation of the energy dependence of the energy-denominator factors appearing in α_{2ph} .

³¹ B. Segall and D. T. F. Marple, *Bull. Am. Phys. Soc.* 11, 189 (1966).

³² E. Gutsche and J. Voigt, in *Proceedings of the International Conference on II-VI Semiconducting Compounds, Providence, R. I.* (W. A. Benjamin, Inc., New York, 1967), p. 337.

their CdS exciton-absorption measurements. This helps explain part of the difference between the calculated and measured values at the higher temperature (i.e., 77°K). It also illustrates the need to properly include the thermal broadening effects in the expressions for the optical transition rates.

To the extent that the spectral dependences can be approximated by (3.12) and (3.14) or that the α_1/α_{2ph} is roughly proportional to Δ over regions of appreciable intensity, the ratio of the total intensity of the one- to the two-phonon emission is proportional to T ; $I_{1LO}/I_{2LO} \approx T/T_0$. This is consistent with the low-temperature intensity data of Gross *et al.*⁴ which are shown in Fig. 8. The value of T_0 obtained from the present calculations is approximately 15°K, while the value determined from Fig. 8 is approximately 6–8°K. This agreement is quite satisfactory considering the uncertainties connected with the background corrections to the data and the limitations on the calculations discussed earlier.

The only available one-LO- and two-LO-phonon-assisted emission data for a material other than CdS are the 77°K data of Packard *et al.*⁶ on ZnO. The luminescence was excited by high-energy electrons. The measured spectrum in the energy range of interest and the calculated emission normalized to the measurements at the peak of the one-LO emission are shown in Fig. 9. The theoretical values were obtained using the calculated absorption coefficient in Ref. 21. The parameters determining the absorption except the effective mass of the hole were determined experimentally and are given in Table I of Ref. 21. The only other parameter needed for the two-LO emission was the average excitation $\langle E_{zn} \rangle - E_{x1}$. This was taken to be the value giving the lower of the two curves in Fig. 12 of Ref. 21, since this provided the better agreement with the 190°K absorption data which are more reliable in the relevant range than the much weaker absorption at lower temperatures. We must also note that the calculation for the absorption was simplified by treating the nearby degenerate *A* and *B* exciton series as a single series with the combined oscillator strength of the two. The agreement with the data is quite satisfactory. Because of the large phonon energy and concomitantly the large sepa-

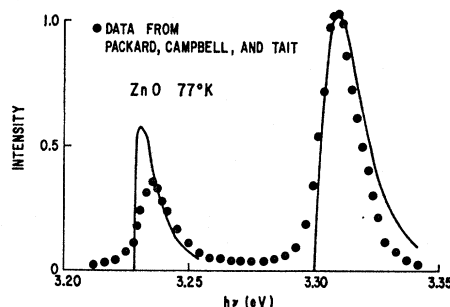


FIG. 9. Calculated one-LO- and two-LO-phonon-assisted fluorescence peaks for ZnO at 77°K compared with the spectrum observed by Packard *et al.*

ration from the zero-LO peak, the polariton effects are not significant for the one-LO peak at this and even much higher temperatures.

In conclusion, it can be seen that the mechanism of LO-phonon-assisted radiative decay of free excitons described in this work⁵ explains all the various aspects of the intrinsic emission below the exciton "resonance" energies. The quantitative results of the present perturbation-theory calculations are found to be in satisfactory accord with the observed spectra considering the scatter between the various reported results and the approximation made in the actual computations. These consist of the neglect of the broadening of the exciton states, which in good crystals is due to exciton-phonon interactions, and of the polariton effects.

ACKNOWLEDGMENTS

We are very grateful to Miss E. L. Kreiger for the numerical computations. We thank Dr. C. E. Bleil for discussion of his spectra and for a preprint, and Dr. W. C. Tait and co-workers for preprints.

APPENDIX A: GREEN'S-FUNCTION TRANSITION RATE IN WEAK-COUPLING LIMIT

A general expression (2.6) was given in Sec. II for the optical transition rate (to lowest order in the exciton-photon interaction) which incorporates the exciton-phonon coupling to all orders. This was derived and expressed in terms of Green's functions. In Secs. III and V, the one-LO-phonon-assisted optical transition rate was evaluated using an equation (3.3) derived by conventional perturbation theory. We now will show how (3.3) is derived from the Green's-function formalism (2.6).

Basically we wish to evaluate the absorption spectra of the process

LO phonon+photon $\rightarrow n=1$ exciton.

The corresponding emission process deduced from (2.8) is

$n=1$ exciton \rightarrow LO phonon+photon.

In the Green's-function formalism, the first quantity one calculates is the self-energy. At low temperatures ($T \ll \omega_l$), it is sufficient to calculate the one-phonon contribution to Σ in order to discuss the one-phonon-assisted optical transition. This self-energy is

$$\Sigma_{\lambda\lambda'}^{(1)}(\mathbf{K}, i\omega_n) = \sum_{\lambda''} \int \frac{d^3q}{(2\pi)^3} V_{\lambda\lambda''}(\mathbf{q}) V_{\lambda''\lambda'}(\mathbf{q}) \times \left(\frac{N_l + 1}{i\omega_n - E_{\lambda''}, \mathbf{K} + \mathbf{q} - \omega_l} + \frac{N_l}{i\omega_n - E_{\lambda''}, \mathbf{K} + \mathbf{q} + \omega_l} \right). \quad (\text{A1})$$

The result $\Sigma_{\lambda}^{(1)}$ is the same except that $\lambda = \lambda'$ in the matrix elements. The only state λ'' whose energy denominator contributes significantly to the absorption

of interest [$\omega < (\epsilon_{\lambda q} - \omega_l)$, for $\lambda \geq 2S$] is the $n=1$ hydrogenic state. Also, only the imaginary part of Σ is important below the exciton resonance line. For $\mathbf{K} = 0$, we can approximate this by ($i\omega_n \rightarrow \omega + i\delta$):

$$-\text{Im}\Sigma_{\lambda\lambda'}^{(1)}(\mathbf{0}, \omega) = \pi N_l \int \frac{d^3q}{(2\pi)^3} \mathcal{U}_0(\mathbf{q}) \mathcal{U}_{\lambda, 1S}(\mathbf{q}) \times \mathcal{U}_{1S, \lambda'}(\mathbf{q}) \delta(\omega - \epsilon_{1S, \mathbf{q}} + \omega_l), \quad (\text{A2})$$

where the exciton kinetic energy is $q^2/2m = \omega + \omega_l - \epsilon_{1S, 0} > 0$, and $\mathcal{U}_0(\mathbf{q})$ is defined and related to the polaron coupling constant α_p by (3.4). We measure our energy zero from the valence band edge.

Using (A2) to obtain $\text{Im}\Sigma_{\lambda}$, we can find $A_{\lambda}(\omega)$, and then the first term in (2.6) contributes

$$\sum_{\lambda} |M_{\lambda}|^2 A_{\lambda} = 2\pi\gamma_0 N_l \sum_{\lambda} \int \frac{d^3q}{(2\pi)^3} \mathcal{U}_0(q) \times \frac{|\psi_{\lambda}(0)|^2 |\mathcal{U}_{\lambda, 1S}(\mathbf{q})|^2 \delta(\omega - \epsilon_{1S, \mathbf{q}} + \omega_l)}{(\omega - \epsilon_{\lambda, 0})^2 + (\text{Im}\Sigma_{\lambda}^{(1)})^2} \quad (\text{A3})$$

to the absorption.

The second term in (2.6) also contributes significantly to the absorption constant. We are interested in terms contributing to W_{abs} which are proportional to the polaron constant α_p ; the terms proportional to α_p^2 are related to the two-phonon processes. Since $\text{Re}\Sigma_{\lambda\lambda'}^{(1)}$ and $\text{Im}\Sigma_{\lambda\lambda'}^{(1)}$ are both proportional to α_p , only the zeroth-order approximation to $A_{\lambda}(\omega)$ and $\text{Re}G_{\lambda}(\omega)$ need to be retained. We then use

$$A_{\lambda}^{(0)}(\omega) = 2\pi\delta(\omega - \epsilon_{\lambda, 0}), \\ \text{Re}^{(0)}G_{\lambda}(\omega) = \text{Re}(\omega - \epsilon_{\lambda 0} + i \text{Im}\Sigma_{\lambda})^{-1} \\ = (\omega - \epsilon_{\lambda, 0}) / [(\omega - \epsilon_{\lambda 0})^2 + (\text{Im}\Sigma_{\lambda}^{(1)})^2].$$

The imaginary part of the self-energy is included in the denominator of $\text{Re}G_{\lambda}(\omega)$, so that the situation in which the energy denominator $\omega - \epsilon_{\lambda, 0}$ is relatively small can be treated and the role of thermal broadening can be exhibited. We can neglect all terms in $A_{\lambda}(\omega)$, since the absorption range of interest is $\omega < \epsilon_{\lambda}$ for all λ . Thus, the only part of the second term in (2.6) which contributes to order α_p is

$$-2 \sum_{\lambda \neq \lambda'} M_{\lambda} M_{\lambda'} \text{Im}\Sigma_{\lambda\lambda'}^{(1)}(\omega) \text{Re}G_{\lambda}(\omega) \text{Re}G_{\lambda'}(\omega) \\ = 2\pi\gamma_0 N_l \sum_{\lambda \neq \lambda'} \int \frac{d^3q}{(2\pi)^3} \mathcal{U}_0(\mathbf{q}) \times \frac{\psi_{\lambda}(0)\psi_{\lambda'}(0)\mathcal{U}_{1S, \lambda}(\mathbf{q})\mathcal{U}_{1S, \lambda'}(\mathbf{q})(\omega - \epsilon_{\lambda, \theta})(\omega - \epsilon_{\lambda', \theta})}{[(\omega - \epsilon_{\lambda 0})^2 + (\text{Im}\Sigma_{\lambda}^{(1)})^2][(\omega - \epsilon_{\lambda', 0})^2 + (\text{Im}\Sigma_{\lambda'}^{(1)})^2]} \\ \times \delta(\omega - \epsilon_{1S, \mathbf{q}} + \omega_l). \quad (\text{A4})$$

The absorption constant is obtained by adding (A3)

and (A4), and we find (restoring \hbar 's)

$$\omega W_{\text{abs}}(\omega) = \frac{2\pi}{\hbar} \gamma_0 N_I \int \frac{d^3q}{(2\pi)^3} \mathcal{U}_0(\mathbf{q}) \times \left| \sum_{\lambda} \frac{\psi_{\lambda}(0) \mathcal{U}_{1S,\lambda}(\mathbf{q})(\omega - \epsilon_{\lambda,0})}{(\omega - \epsilon_{\lambda,0})^2 + (\text{Im}\Sigma_{\lambda}(1))^2} \right|^2 \delta(\hbar\omega - \epsilon_{\lambda,\mathbf{q}} + \hbar\omega_I). \quad (\text{A5})$$

With the neglect of the damping term in the denominator, this is the same result as the conventional perturbation-theory, or Golden rule, formula (3.3). This shows that the two methods are equivalent in the weak-coupling limit except for damping effects. The more general result, obtained by the Green's-function method, should be used when the damping constants in the energy denominators cannot be ignored.

APPENDIX B: ESTIMATE OF DEPENDENCE OF TRANSITION RATE FOR TWO-LO-ASSISTED PROCESSES ON ANISOTROPY

As indicated in Sec. III C, around the threshold for the two-LO processes (more precisely, when $\Delta_2 \ll \mu B/M$) only values of $\mathbf{q} \approx -\mathbf{q}'$ contribute to the sixfold integrals

$$I_2 = \int d^3q \int d^3q' |\{\mathbf{q}, \mathbf{q}'\}|^2,$$

where $\{\mathbf{q}, \mathbf{q}'\}$ is defined in Eqs. (23) and (25) of Ref. 12. Even at somewhat higher $\hbar\omega$, this region of $(\mathbf{q}, \mathbf{q}')$ space makes the major contribution to α_{2ph} . To study the dependence on anisotropy, it suffices then to set $\mathbf{q} = -\mathbf{q}'$ in $\{\mathbf{q}, \mathbf{q}'\}$. Further, it is found that for all values of $\mathbf{q} \approx -\mathbf{q}'$ the terms with the factor $\langle 1 | U(\mathbf{q}) U(\mathbf{q}') | 1 \rangle$ are appreciably larger than the other terms, which we consequently

neglect for this estimate. The integral over \mathbf{q}' yields the density of states $4\pi(2M_1^2 M_{11})^{1/2} \Delta_2^{1/2}$. We find

$$J_2 = [4\pi(2M_1^2 M_{11})^{1/2} \Delta_2^{1/2}]^{-1} I_2 = \int \frac{d^3q}{q^4} \times \frac{\{1 - [1 + (q_{11}^2 + q_{11}^2 m_{hL} M_{11} / m_{h11} M_1)(a/2)^2]^{-2}\}^2}{(\langle E_{xn} \rangle + q^2 / 2M_1 + q_{11}^2 / 2M_{11} - \hbar\omega_I - \hbar\omega)^2}.$$

We note that since m_e is significantly less than m_{hL} and m_{h11} for the materials of interest, the coefficient of q_{11}^2 in the curly brackets is unity to within about 20%. Further, since the major contribution to the integral comes from $qa \lesssim 1$, the possible variation in I_2 due to the anisotropy factor in this term can only be a few percent. We thus set this factor equal to unity. Carrying out the angular integration we obtain

$$J_2 = \frac{2\pi a}{B^2} \int_0^\infty \frac{dy}{y^2} \frac{\{1 - [1 + (y/2)^2]^{-2}\}^2}{F(y)} \times \left\{ \frac{1}{G(y)} + \frac{1}{2y\gamma F(y)} \ln \left[\frac{[F(y)]^{1/2} + y\gamma}{[F(y)]^{1/2} - y\gamma} \right] \right\},$$

where

$$\gamma^2 = \mu(M_{11} - M_1) / M_1 M_{11},$$

$$F(y) = (\langle E_{xn} \rangle - E_{x1} + \hbar\omega) B^{-1} - \mu y^2 / M_1,$$

and

$$G(y) = (\langle E_{xn} \rangle - E_{x1} + \hbar\omega) B^{-1} - \mu y^2 / M_{11}.$$

This integral has been evaluated for $M_{11} = 2$ and 8 using the $M_1 = 1$ and $(\langle E_{xn} \rangle - E_{x1}) B^{-1} = 2$ and 5. The variation over this large range of M_{11} (or m_{h11}) was less than 8%. In contrast, the density-of-states factor varies by a factor of 2 and $\alpha_{1ph}(\hbar\omega)$ near threshold by almost a factor of 3 over this range of M_{11} .